Supporting Information

Leong et al. 10.1073/pnas.1413886112

SI Materials and Methods

Antibodies. The following antibodies were used: from BD Biosciences, NK1.1 (PK136), NKp46 (29A1.4), CD45 (30-F11), CD3 (2C11), CD11b (M1/70), CD62L (MEL-14), CD2 (RM2-5), CD8 (53-6.7), CD19 (1D3), Gr-1 (RB6-8C5), Ter-119 (Ter-119), CD44 (IM7), IFNγ (XMG1.2), CD51 (RMV-8), CD49b (DX5), CD43 (S7), CD122 (TM-β1), Ly49C/I (5E6), Ly49F (HBF-719), Ly49D (4E5), Ly49G2 (4D11), CD69 (H1.2F3), p-AKT (S473, M89-61), p-AKT (T308), and p-ERK1/2 (pT202/pY204); from R&D, CCR1 (643854), CCR2 (475301), and CCR5 (HM-CCR5); from eBioscience, CD27 (LG.3A10), NKp46 (29A1.4), CXCR3 (173), CXCR4 (2B11), CD107a (1D4B), CD94(18D3), NKG2A/C/E (20d5), NKG2D (CX5), Ly49H (3D10), and KLRG1 (2F1); from Biolegend, CD45.1 (A20), CD45.2 (104), CD49d (R1-2), LFA-1 (H155-78), and Ly49A (A1); and from Cell Signaling Technologies, p-mTOR (S2448, D9C2), p-4EBP1 (T37/46, 236B4), p-S6 (S371), p-S6 (T389), and anti-rabbit IgG $F(ab')_2$ (no. 8885).

Cytokine Production and Degranulation Assays. We incubated 1×10^6 splenocytes in complete RPMI containing IL-12 (10 ng/mL) + IL-15 (100 ng/mL), IL-12 (2 ng/mL) + IL-18 (20 ng/mL), or on plates precoated with anti-NK1.1 antibody (coated for 90 min at 37 °C at 5 μg/mL). At the start of the assay, anti-CD107a antibody was added to wells containing anti-NK1.1 antibody. After 1 h, Brefeldin A and Monensin were added and incubated for an additional 5 h. Cells were surface stained, fixed and permeabilized (BD Cytofix/Cytoperm), stained for NK cell markers, and analyzed by flow cytometry.

Phosphoprotein Flow Cytometry. NK cells were surface stained 15 min before adding an equal volume of prewarmed 4% formaldehyde. After fixation for 10 min, cells were permeabilized with Perm buffer III (BD) for 30 min on ice. Permeabilized cells were washed three times with FACS buffer (PBS, 1 mM EDTA, 2% FBS) and intracellular stained for 1 h at 25 °C. Cells were washed three times with FACS buffer and analyzed by flow cytometry.

Western Blotting. FACS-purified YFP^+ NK cells were immediately lysed in RIPA buffer with protease inhibitors (Roche) to obtain protein lysates. Lysates were resolved on an SDS/PAGE gel and probed using an anti-mouse PTEN antibody (D4.3, Cell Signaling Technology) and anti–β-actin antibody (C4, Santa Cruz Biotechnology) as a loading control.

RT-PCR and Quantitative RT-PCR. RNA from FACS-sorted YFP+ cells were isolated using TRIzol. Total cDNA was generated with the High-Capacity cDNA Reverse Transcription kit (Life Technologies). The following primers were used for identification of loxp flanked (576 bp) or excised (303 bp) *pten* exon 5: F, tgacgtgttcccttcatgca; R, tggtccacaaagagggagga. SYBR green real-time PCR was performed on cDNA generated from DNase-treated RNA using the High-Capacity Reverse Transcription Kit (Applied Biosystems). PCR was completed on an ABI StepOne Plus instrument. The primers used are as follows: S1P1 F, ACTTTGCGAGTGAGCTGGTC; S1P1 R, TTTTCCTTGG-CTGGAGAGG; S1P5 F, ACACCAAATGCCCAGCTTAC; S1P1 R, TGGAGCACTGTGCAAAAGTC. 18S rRNA was used as a housekeeping control (Taqman Ribosomal RNA control, Life Technologies) and amplified using TaqMan Fast Advanced Master Mix (Life Technologies).

Caspase Activation Assay. Pan-caspase (FLICA) assays were completed using the Vybrant FAM poly-caspase kit (Life Technologies) according to the manufacturer's instructions.

Immunostaining and Preparation of BM Sections. Femurs were removed and fixed in 4% paraformaldehyde overnight at 4 °C. Bones were decalcified in 14% EDTA for 3 d at 4 °C. Bones were cryopreserved in 30% sucrose, embedded in OCT media, and frozen. We cut 50-μm sections using Leica Cryostat and dried them for 2 d at room temperature. Sections were blocked in 10% donkey serum and stained with chicken anti-GFP (Abcam), rat anti-B220 (eBioscience), and rat anti-endomucin (eBioscience) followed by anti-rat IgG conjugated to Dylight 650 (Abcam) and anti-chicken IgY (IgG)+(H+L) conjugated to Alexa Fluor 488 (Jackson ImmunoResearch). Nuclei were counterstained with DAPI. Whole-mount images were acquired using Zeiss LSM 700 confocal microscope, and images were analyzed using Zen (Zeiss) and Volocity (Perkin-Elmer) software.

Immunostaining and Preparation of Spleen and LN Sections. Spleens and LNs were harvested from mice, then fixed and dehydrated overnight (4% paraformaldehyde, 30% sucrose, PBS pH 7.4) at 4 °C with constant agitation. Tissues were embedded in Tissue-Tek (Sakura Finetek) over dry ice and stored at –80 °C. Cryostat sections were cut 9-μm thick and rehydrated in PBS. Sections were incubated with 2.4G2 "Fc block" hybridoma supernatant (rat IgG2b kappa) for 15 min. Sections were then incubated with fluorescently conjugated antibodies for 1 h, rinsed in PBS, and mounted in VECTASHIELD HardSet Mounting Medium with DAPI (Vector Labs). Antibodies used included anti–B220-phycoerythrin (PE) (clone RA3-6B2 from eBiosciences) and anti–CD3e-allophycocyanin (APC) (clone 145–2C11 from eBiociences). Images were acquired using a Nikon Eclipse 80i microscope (100× magnification) and processed using MetaMorph (Molecular Devices).

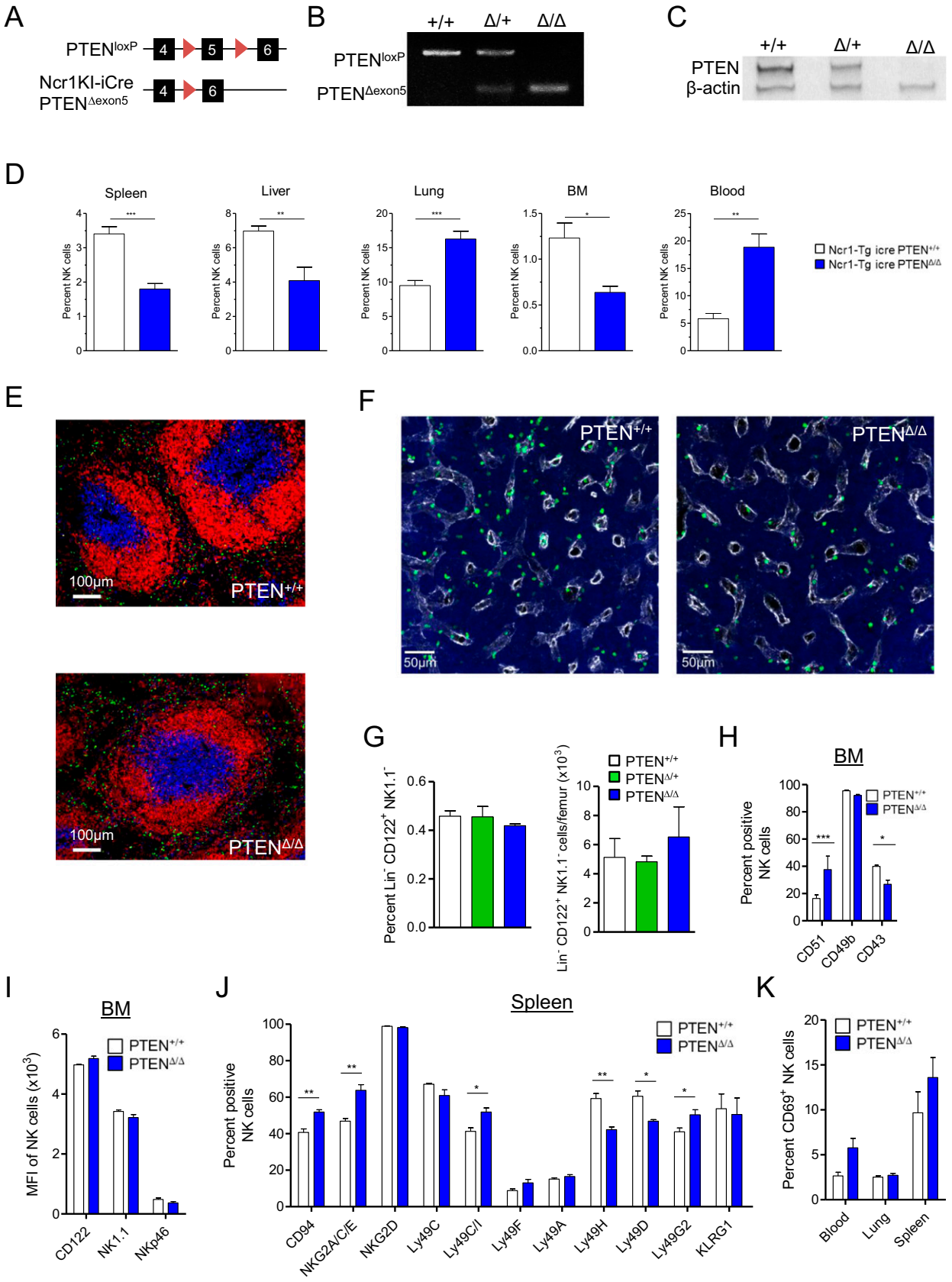

Fig. S1. NK-specific deletion of the phosphatase domain of *pten* results in loss of PTEN expression and alterations in the expression of NK cell developmental markers. (*A*) Exon 5 of PTEN is flanked by loxP sites and is excised in the presence of Cre driven by Ncr1 expression. (*B*) RT-PCR analysis of YFP^{+} splenic NK cells purified from Ncr1 knock-in iCre ROSA26 YFP$^{loxP/stop/loxP}$ PTEN$^{+/+}$, PTEN$^{\Delta/+}$, or PTEN$^{\Delta/\Delta}$ mice shows excision of *pten* exon 5 concordant with YFP and Cre ex-

Legend continued on following page

pression. (*C*) Western blot against PTEN in purified YFP$^+$ PTEN$^{+/+}$, PTEN$^{\Delta/+}$, and PTEN$^{\Delta/\Delta}$ NK cells demonstrates protein loss in the PTEN$^{\Delta/\Delta}$ genotype. (*D*) Ncr1-Tg iCre PTEN$^{\Delta/\Delta}$ display similar abnormalities in NK cell distribution. Ncr1-Tg iCre mice were bred to Rosa YFP reporter and PTEN$^{flox/flox}$ mice to generate Ncr1-Tg iCre Rosa-LSL-YFP PTEN$^{\Delta/\Delta}$ mice. NK cell frequency was calculated as the percentage of YFP$^+$ CD3$^-$ cells in lymphocytes. (*E*) Immunofluoresence staining of the spleen reveals no overt defects in NK cell localization of PTEN$^{\Delta/\Delta}$ mice. Frozen sections were visualized by YFP (green), CD3 (blue), and B220 (red). (*F*) Immunofluoresence staining of BM reveals no overt defects in NK cell localization of PTEN$^{\Delta/\Delta}$ mice. Frozen sections were visualized by YFP (green), DAPI (blue), and endomucin (white). (*G* and *H*) BM isolates from mouse femurs were stained for lineage (CD3, CD8, CD19, Gr-1, Ter-119) CD122$^+$ NK1.1$^-$ cells. The NK precursor frequency and number, calculated by multiplying the frequency by total femur cell number, is shown. (*H* and *I*) Flow cytometric analysis of the expression of various BM NK cell (defined by YFP$^+$ CD3$^-$ expression) markers. (*J*) Flow cytometric analysis of the expression of various splenic NK cell (defined by YFP$^+$ CD3$^-$ expression) markers. (*K*) Expression of CD69 on NK cells from different lymphoid compartments. Data shown in *B* and *C* are representative of two independent experiments. Data shown in *D* are mean ± SEM of four independent experiments with $n = 7$ mice for each genotype. Data shown in *E* and *F* are representative of 2–3 mice. Data shown in *G–K* summarize results of 3–4 mice in two independent experiments and are shown as mean ± SEM.

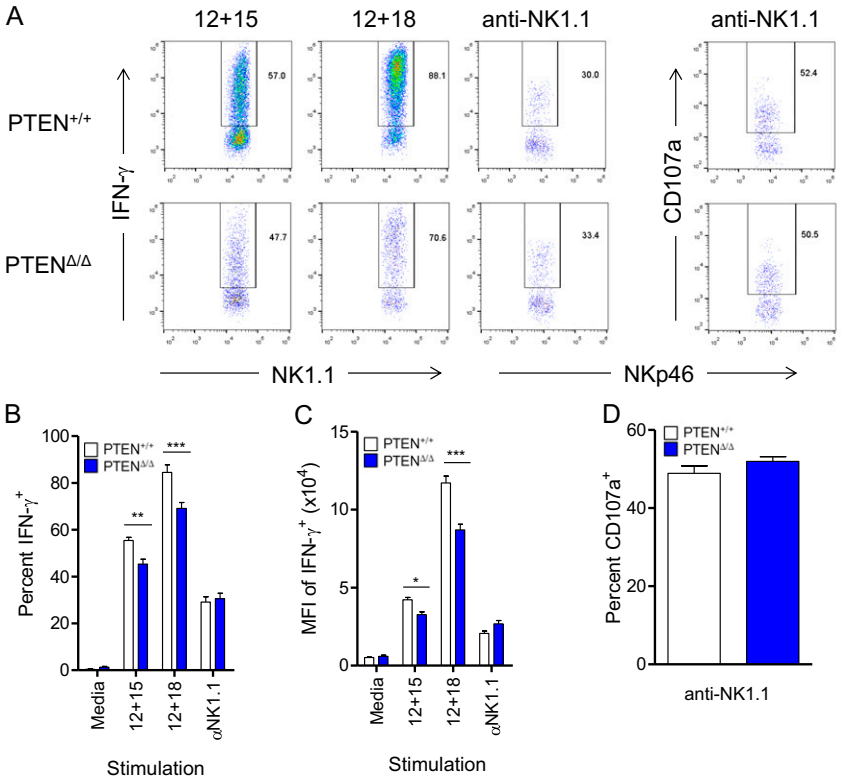

Fig. S2. PTEN$^{\Delta/\Delta}$ NK cells produce less IFN-γ in response to cytokine stimulation but not activating receptor ligation. (*A*) Splenocytes were cultured for 6 h with IL-12 + IL-15, IL-12 + IL-18, or on microtiter plates coated with anti-NK1.1 ligating antibody. After 6 h, splenocytes were stained for NK cell markers, intracellular IFN-γ, and the presence of surface CD107a. The bivariate plots shown are mean ± SEM of six mice in two independent experiments, summarized in *B–D*.

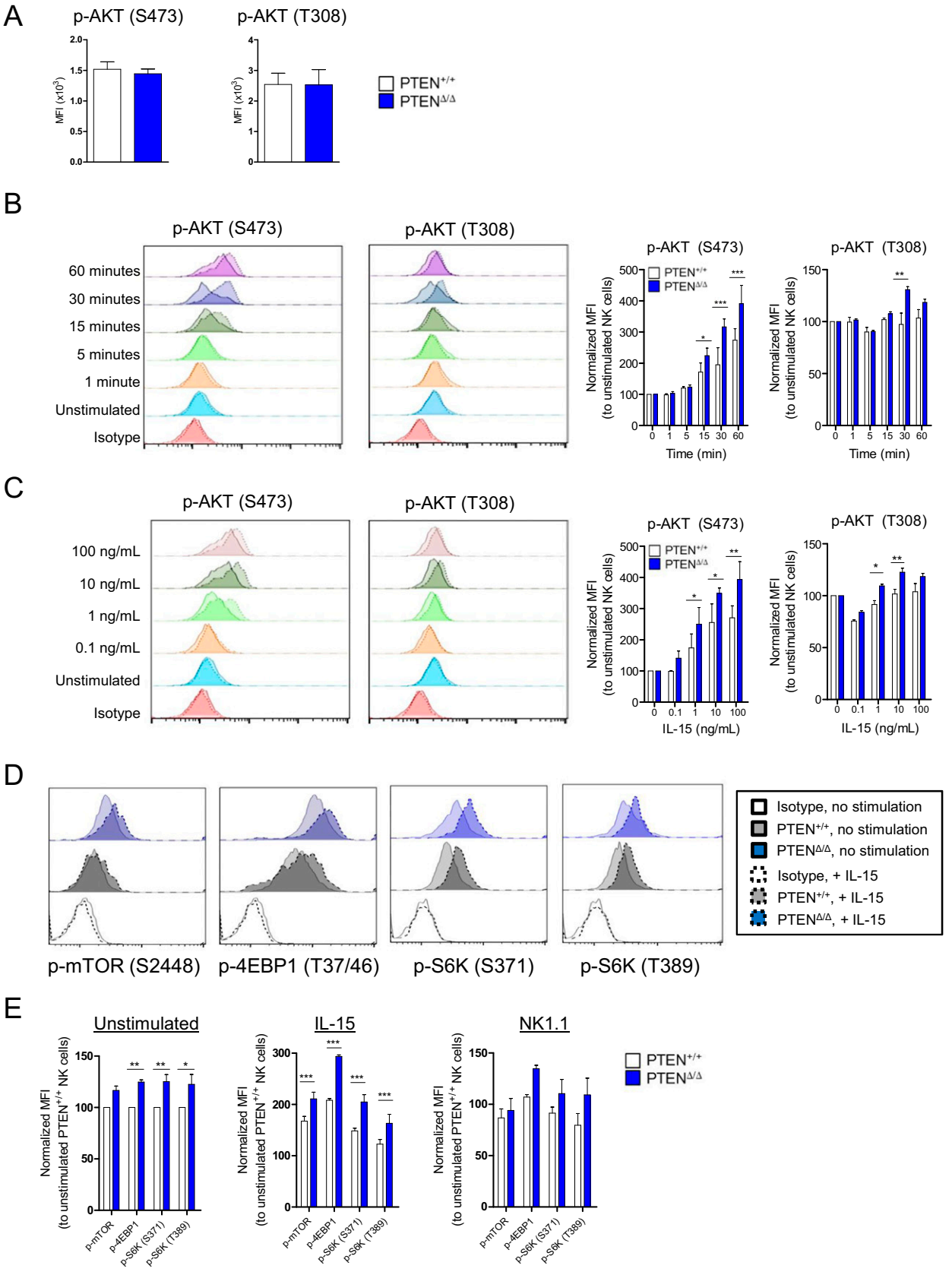

Fig. S3. PTEN deletion results in enhanced mTOR activity with and without exogenous IL-15 stimulation. (*A*) PTEN$^{+/+}$ and PTEN$^{\Delta/\Delta}$ splenic NK cells were freshly isolated and stained for p-AKT expression as described in *SI Materials and Methods*. (*B*) Splenic NK cells were stimulated with 10 ng/mL IL-15 for the indicated time and stained for p-AKT. Shown are PTEN$^{+/+}$ NK cells (solid line) and PTEN$^{\Delta/\Delta}$ NK cells (dashed line). (*C*) Splenic NK cells were stimulated for 1 h with the

Legend continued on following page

indicated dose of IL-15. (*D*) Splenic NK cells were either stained with antibodies against p-mTOR, p-4EBP1, or p-S6 after culture in either media or 10 ng/mL IL-15 for 1 h. (*E*) Summary data showing increased phosphorylation of downstream mTOR substrates at baseline. Following IL-15 stimulation but not NK1.1 stimulation, further increases in mTOR substrate phosphorylation were observed. Data in *A*–*E* are mean ± SEM of 3–4 mice of each genotype in three independent experiments.

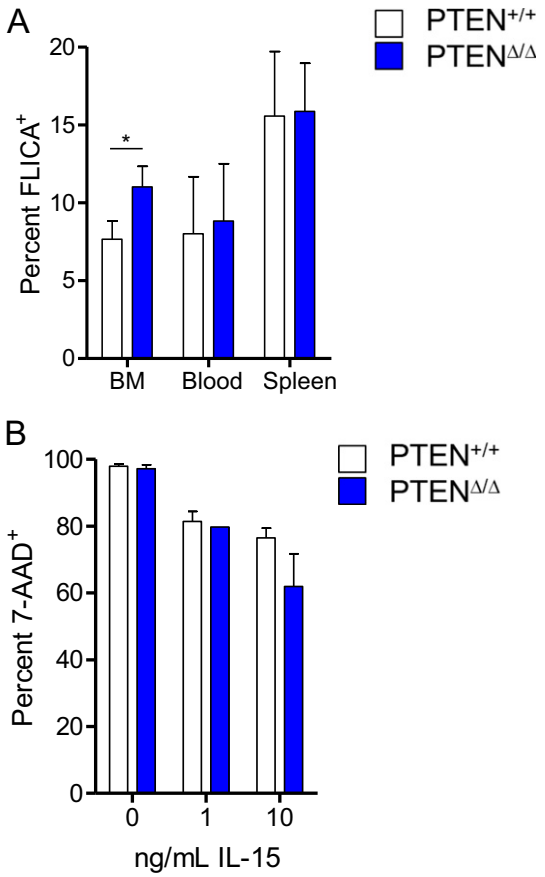

Fig. S4. Ex vivo survival of splenic NK cells in low-dose IL-15 culture is not affected by PTEN loss, and caspase activation is modestly increased in BM PTEN$^{\Delta/\Delta}$ NK cells. (*A*) Caspase activation was determined in freshly isolated BM, blood, or spleen NK cells as described in *SI Materials and Methods*. Data are mean ± SEM of three mice of each genotype in two independent experiments. (*B*) Isolated splenocytes were cultured for 7 d in media containing varying doses of mouse IL-15. Half-media changes and cytokine replenishment was performed every other day. 7-AAD staining was assessed by flow cytometric analysis on day 7 on gated NK1.1^{+} CD3^{-} cells. Data are mean ± SEM of 2–4 mice of each genotype in two independent experiments.

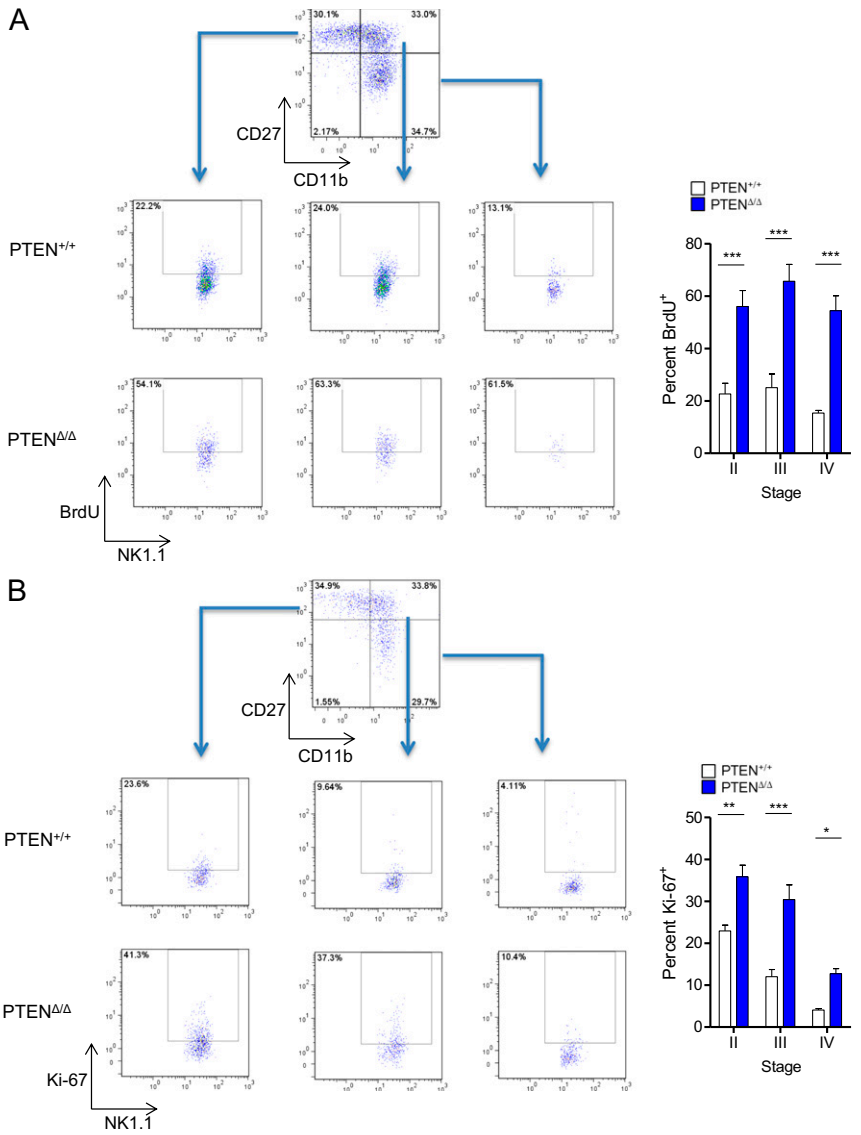

Fig. S5. Increased proliferation in PTEN$^{\Delta/\Delta}$ NK cells is independent of maturation stage. (*A*) BM cells from PTEN$^{+/+}$ or PTEN$^{\Delta/\Delta}$ mice injected with BrdU twice a day for 3 d were analyzed for BrdU incorporation within each NK cell CD27/CD11b maturation stage. (*B*) BM cells from PTEN$^{+/+}$ or PTEN$^{\Delta/\Delta}$ mice were assessed for K_i-67 expression within each NK cell CD27/CD11b maturation stage. Summary data are mean ± SEM of four mice in two independent experiments.

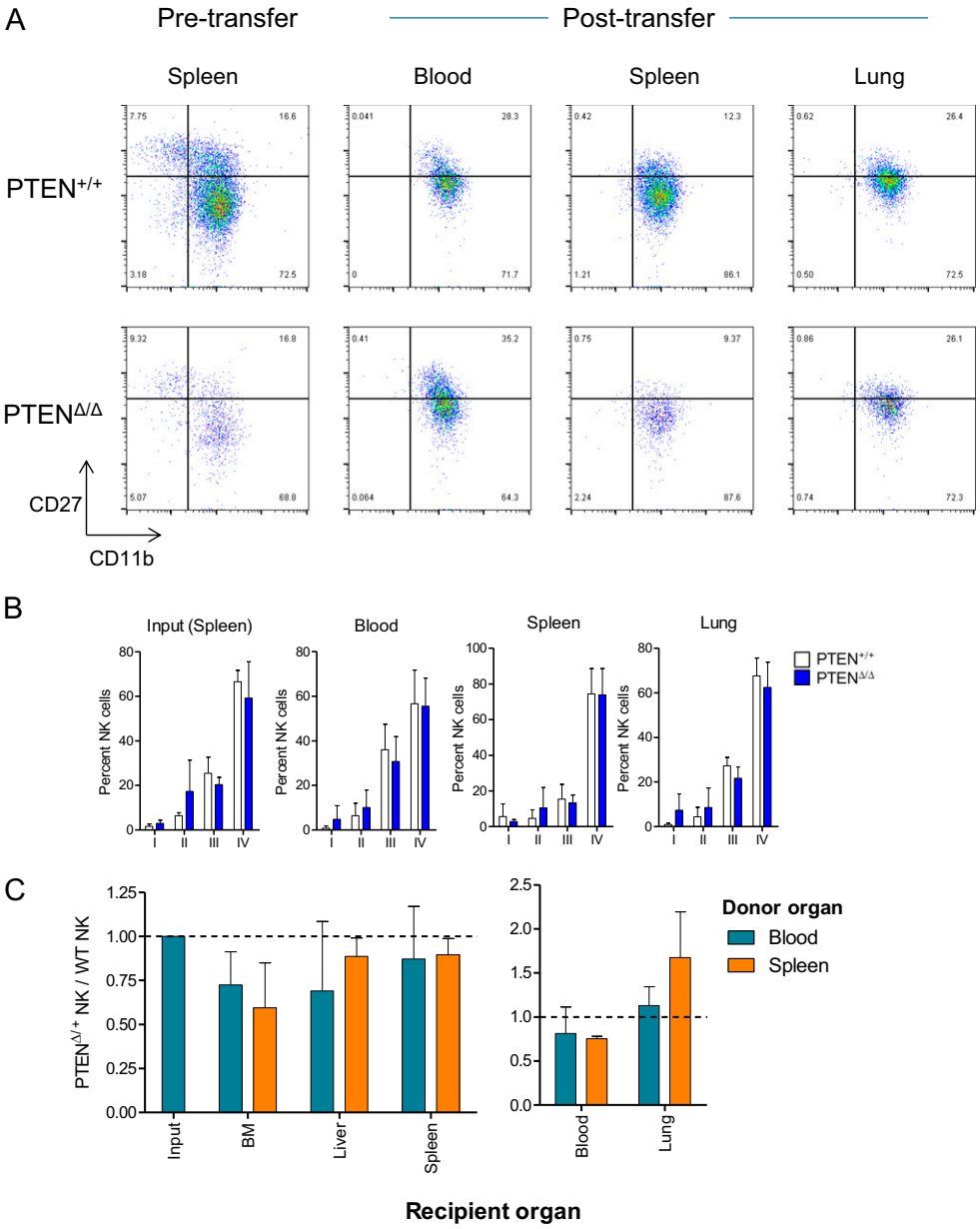

Fig. S6. Maturation profiles of NK cells transferred from PTEN$^{+/+}$ and PTEN$^{\Delta/\Delta}$ are similar, and PTEN$^{\Delta/+}$ NK cells do not have a significant defect in trafficking. (*A* and *B*) Splenocytes were transferred into non-YFP–expressing wild-type mice and killed after 16 h as described in *Materials and Methods*. Donor NK cells in isolated peripheral blood, spleen, or lung were identified by YFP expression and stained with antibodies against CD27 and CD11b. Summary data are mean ± SEM of four mice performed in four independent experiments. (*C*) Spleen or blood PTEN$^{\Delta/+}$ and PTEN$^{+/+}$ NK cells were competitively transferred into wild-type recipients, and the indicated lymphoid compartments were analyzed for relative frequency of donor NK cells after 16 h. Summary data are mean ± SEM of 2–3 mice in two independent experiments.

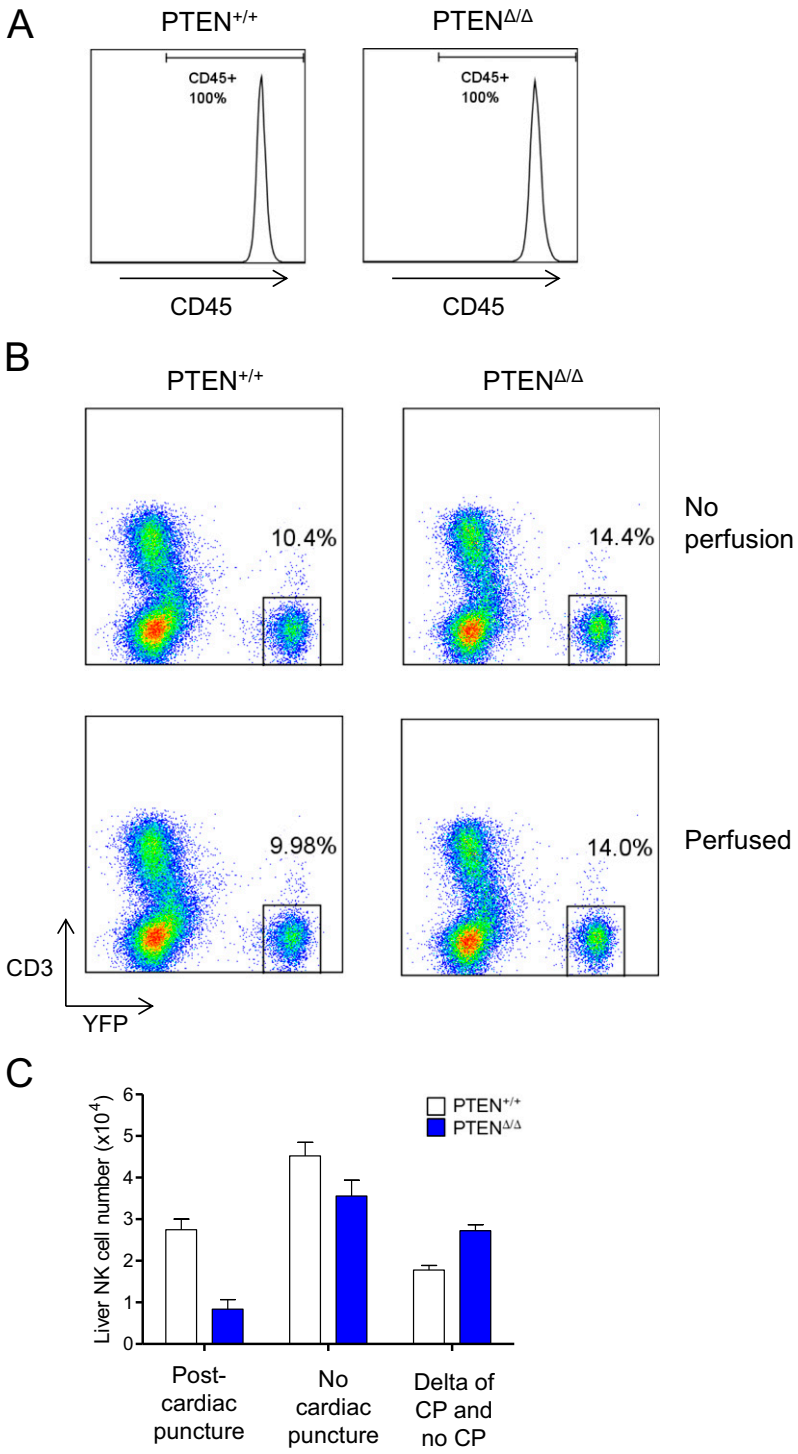

Fig. S7. PTEN$^{\Delta/\Delta}$ NK cells are elevated in lung and liver sinusoids. (*A*) Mice were injected with anti-CD45 antibody, killed after 5 min, and the lungs processed into single cell suspensions. Representative histograms of gated YFP+ CD3– NK cells show exclusive anti-CD45 labeling. (*B*) In separate experiments, mice were perfused with 10 mL PBS by intraventricular puncture before lung isolation and analysis for NK cell frequency. (*C*) PTEN$^{\Delta/\Delta}$ liver contains elevated NK cell numbers in the peripheral blood pool. Mice were either untreated or cardiac punctured to remove circulating blood before liver processing, as described in *Materials and Methods*. Liver single cell suspensions were stained for NK cell markers and counted using flow cytometry counting beads. The difference in liver NK cell numbers between mice receiving cardiac puncture or not is the peripheral blood NK cell pool in the liver, shown in the right-most column set. Data are mean ± SEM from four mice in two independent experiments.

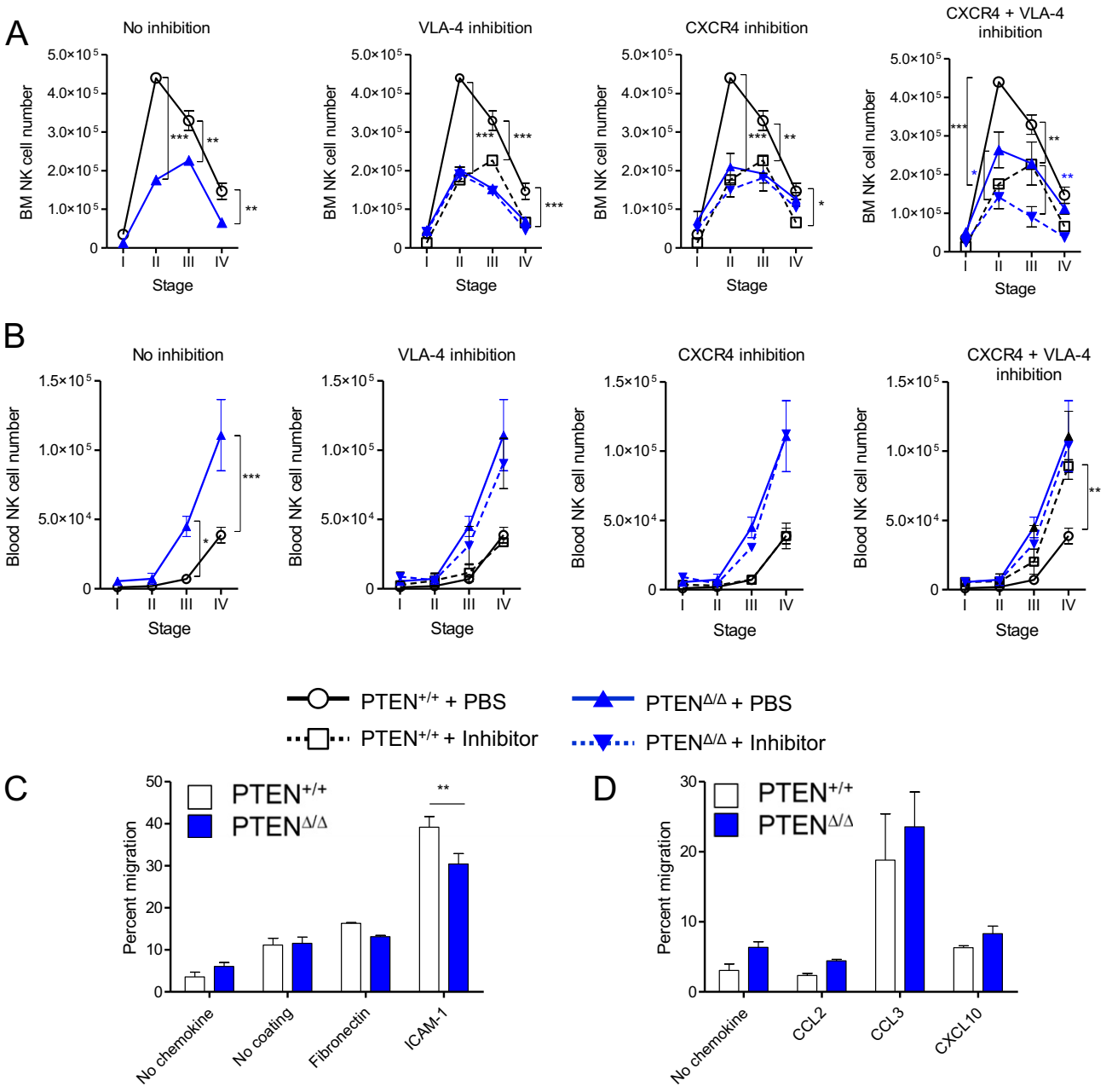

Fig. S8. PTEN$^{\Delta/\Delta}$ NK cells are unresponsive to CXCR4 and VLA-4 inhibition in vivo, and PTEN$^{\Delta/\Delta}$ mice have no defects in chemotaxis to CCL2, CCL3, or CXCL10, but are retained in migration across ICAM-1–coated transwells. (*A*) PTEN$^{+/+}$ or PTEN$^{\Delta/\Delta}$ mice were treated with saline, firategrast i.v., AMD3100 i.p., or firategrast and AMD3100 together for 1 h before sacrifice. The (*A*) BM and (*B*) peripheral blood NK cells were analyzed by CD27/CD11b maturation stages. Data are mean ± SEM of two independent experiments using 12 PTEN$^{+/+}$ or PTEN$^{\Delta/\Delta}$ mice. Significance is shown comparing PTEN$^{+/+}$ to PTEN$^{\Delta/\Delta}$ NK cell numbers (no inhibition) or untreated to inhibitor-treated NK cell numbers (single and combined inhibitor treatments). (*C*) Transwells were precoated with fibronectin or ICAM-1 at 5 μg/mL for 90 min. Splenocytes were then added to the top well and allowed to migrate for 3 h into the lower transwell containing 10 ng/mL CXCL12 in RPMI + 4 mg/mL fatty acid-free BSA. Data shown are mean ± SEM representing three mice in two independent experiments. (*D*) Uncoated transwell assays were performed as described in *Materials and Methods*. The lower transwell contained RPMI + 4 mg/mL fatty acid-free BSA and 10 ng/mL CCL2, CCL3, or CXCL10. Data shown are mean ± SEM representing 3–7 mice in two independent experiments.

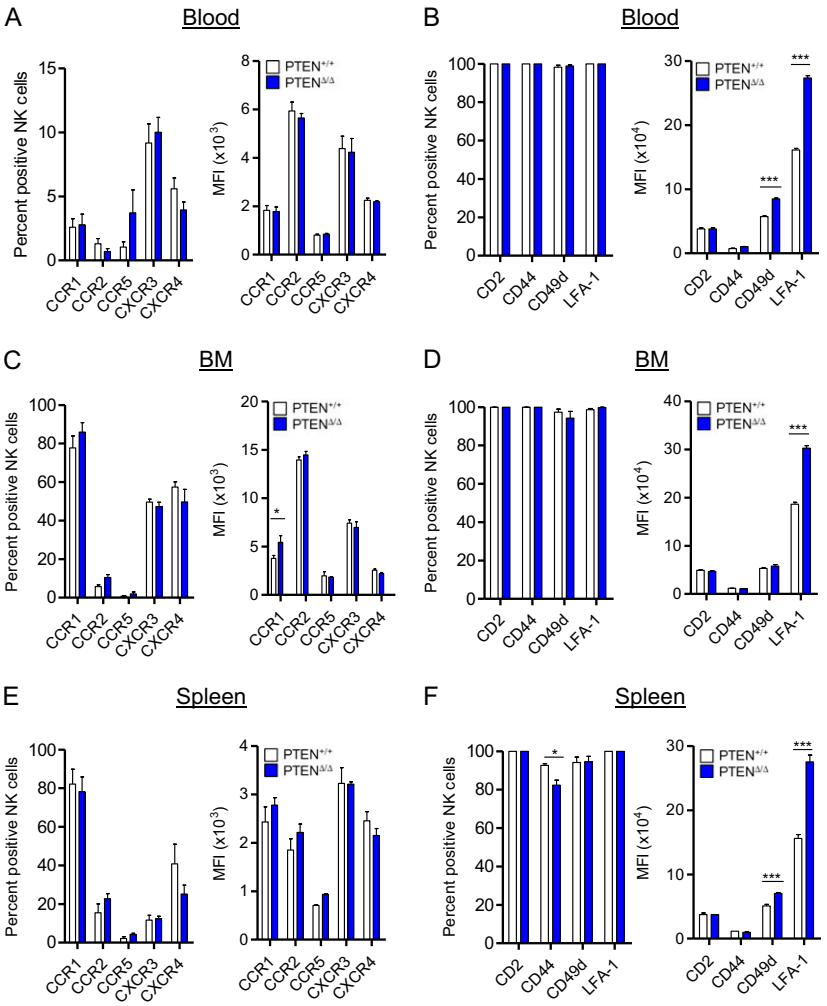

Fig. S9. Flow cytometric analysis of chemokine and integrin receptor expression reveals up-regulation in VLA-4 and LFA-1. The (*A* and *B*) blood, (*C* and *D*) bone marrow, or (*E* and *F*) spleen of PTEN$^{+/+}$ or PTEN$^{\Delta/\Delta}$ mice were stained for YFP^{+}CD3^{-} expression and various chemokine and integrin receptors. Data shown are mean ± SEM representing 3–8 mice per summary graph.